DNA Repair 113 (2022) 103300

Contents lists available at ScienceDirect

DNA Repair

journal homepage: www.elsevier.com/locate/dnarepair

The rate of formation and stability of abasic site interstrand crosslinks in the DNA duplex

Andrea Huskova [1], Barbora Landova [1], Evzen Boura, Jan Silhan [*]

Institute of Organic Chemistry and Biochemistry of the Czech Academy of Sciences, Flemingovo namesti 2, 166 10 Prague 6, Czech Republic

ARTICLE INFO

Keywords:
DNA damage
Interstrand crosslink
Abasic site
Non-enzyme kinetics
DNA repair

ABSTRACT

DNA interstrand crosslinks (ICLs) strands pose an impenetrable barrier for DNA replication. Different ICLs are known to recruit distinct DNA repair pathways. NEIL3 glycosylase has been known to remove an abasic (Ap) site derived DNA crosslink (Ap-ICL). An Ap-ICL forms spontaneously from the Ap site with an adjacent adenine in the opposite strand. Lack of genetic models and a poor understanding of the fate of these lesions leads to many questions about the occurrence and the toxicity of Ap-ICL in cells.

Here, we investigate the circumstances of Ap-ICL formation. With an array of different oligos, we have investigated the rates of formation, the yields, and the stability of Ap-ICL. Our findings point out how different bases in the vicinity of the Ap site change crosslink formation *in vitro*. We reveal that AT-rich rather than GC-rich regions in the surrounding Ap site lead to higher rates of Ap-ICL formation. Overall, our data reveal that Ap-ICL can be formed in virtually any DNA sequence context surrounding a hot spot of a 5′-Ap-dT pair, albeit with significantly different rates and yields. Based on Ap-ICL formation *in vitro,* we attempt to predict the number of Ap-ICLs in the cell.

1. Introduction

Interstrand DNA crosslinks (ICLs) are a type of DNA damage in which opposite DNA strands are covalently linked. ICLs form an impenetrable barrier that prevents DNA replication [1]. Various forms of ICLs that differ both structurally and chemically have been identified [2–5]. To combat the deleterious and toxic consequences of these lesions, distinct DNA repair mechanisms have evolved. At present, two distinct DNA repair processes have been identified. The first repair process is the NEIL3 pathway involving NEIL3 glycosylase, and the second is the Fanconi Anaemia DNA repair pathway (FA pathway) [6,7]. These two pathways are intrinsically linked to DNA replication and complement each other in the repair of ICLs. The NEIL3 pathway has been linked to an early stage of replication coupled repair when replication forks stall on the crosslink and is known for the removal of abasic site ICLs (Ap-ICLs) [4,8]. Additionally, NEIL3 is also involved in the recognition and excision of psoralen-induced ICLs. The same ability has also another glycosylase, NEIL1. Importantly, the excision activity of these glycosylases doesn't generate double-strand breaks [9]. The later recruited FA pathway recognises and repairs crosslinks arising from small aldehydes such as acetaldehyde derived crosslinks. It has been identified and it is known for its ability to repair DNA crosslinks generated from exogenous crosslinking compounds, used as chemotherapeutics or in warfare (*e.g.* cis-platin and nitrogen mustard) [10–12].

An abasic site (apurinic/apyrimidinic), or an Ap site, can be generated spontaneously in large quantities, as it was estimated that 10,000 Ap sites form per cell every day [13,14]. This astronomical number is increased even further, mainly by some DNA glycosylases that remove damaged bases from the genome [15]. One of the most well-known is Uracil DNA glycosylase, an important enzyme not only in base excision repair but also in somatic hypermutation during the diversification of antibodies [16–19]. It removes uracil, generated either by spontaneously or enzymatic deamination of cytosine. The Ap site undergoes spontaneous or enzymatic cleavage. The Ap endonucleases cleave the phosphodiester bond of the Ap site while producing a nick with 3′-deoxyribose-5′-phosphate and a single-strand DNA (ssDNA) break [20,21]. Two groups of Ap lyases cleave the Ap site either *via* β-elimination generating an unsaturated 3′-aldehyde or through the β-δ

Abbreviations: Ap site, apurinic/apyrimidinic site, abasic site in DNA; ICL, Interstrand DNA crosslink; NEIL3, nei-like DNA glycoslase 3.

* Corresponding author.
E-mail address: silhan@uochb.cas.cz (J. Silhan).

[1] These authors contributed equally to this work

https://doi.org/10.1016/j.dnarep.2022.103300
Received 7 January 2022; Received in revised form 8 February 2022; Accepted 8 February 2022
Available online 11 February 2022

elimination to yield 3′-phosphate [22,23]. The Ap site also undergoes spontaneous breakage with a half-life of 8 days, and the rate can be enhanced by basic hydrolysis catalysed by amines or an increase of pH. First, the Ap site undergoes β-elimination followed by δ-elimination with 3′-phosphate as the final endproduct [24,25]. These toxic 3′-lesions block ligation and replication and are generally repaired by specific 3′-phosphates, such as PNK or Ap exonucleases [26–29]. Finally, the generated ssDNA break with 3′-OH is repaired by a DNA polymerase and ligase [25,30,31]. A nucleophilic attack of the Ap site may form a DNA interstrand crosslink or a DNA-protein crosslink [4,32].

From a chemical point of view, an Ap site undergoes structural changes, such as mutarotation and spontaneous decomposition [33]. Spontaneous base loss is caused by hydrolysis where the C1 of deoxyribose is attacked by a water molecule from the opposite side of the N-glycosidic bond [30]. This reaction leads to the formation of an Ap site with an alpha-OH group at C1. Further on the Ap site, it undergoes mutarotation until the thermodynamic equilibrium is reached [33,34]. Interestingly, this process reaches equilibrium when only 1% of the ribose ring opens to its aldehyde form [33,35]. Aldehydes are reactive groups that readily interact with amines, forming a relatively stable covalent imine commonly known as a Schiff base [36–38].

Very early on, it was suggested that the Ap site can generate ICL in double-stranded DNA [39,40]. This was later confirmed and further investigated in several publications [41–43]. Most of these experiments were carried out at relatively low pH, somewhat harsh and non-physiological conditions. Nonetheless, one rough estimate at pH = 6.8 in T7 phage DNA was that 1 crosslink is formed per 140 Ap sites [40]. Eventually, the nature of the chemical agent responsible for crosslink formation on the Ap site was found to be the aldehyde group, and the optimum for Ap-ICL formation is in the low pH region [44].

Successfully reconstituted Ap-ICL at a specific site *in vitro* was accomplished for the Ap site crosslinking with guanine in an opposite DNA strand within the 5′-dC-Ap sequence [4]. These crosslinks were formed under relatively acidic conditions (pH = 5) and stabilized by the reduction with sodium cyanoborohydride ($NaBH_3CN$) and characterized by mass spectroscopy. Shortly thereafter, another Ap-ICL was discovered where the Ap site linking with opposing adenine downstream of the Ap site, and therefore a different sequence context (5′-ApT) was confirmed. This Ap-ICL was shown to be stable, and it formed under physiological conditions [46]. A subsequent NMR study confirmed that one of the Ap-ICLs generated between ApT:A is attached with the N6-amino group of the dA from the opposite strand [47]. In this study, Ap-ICL was extracted from the duplex by enzymatic digestion and analysed by NMR. The presence of different sugar moiety isomers was found in equilibrium. The latest NMR study reveals that the structure of Ap-ICL has the Ap site's ribose ring closed in its furanose form [45]. In this work, the DNA contains a 5′-dC-Ap-dT sequence (Fig. 1).

These studies have sparked questions regarding the repair of these Ap-ICLs in the cell. The first repair that was discovered is linked to replication and is orchestrated by the DNA glycosylase NEIL3 [7]. Subsequently, it was demonstrated that this enzyme requires a replication fork with a specific orientation of the Ap part of the lesion to be catalytically efficient. Furthermore, NEIL3 is recruited to the ICL by TRAIP1 dependent ubiquitylation of DNA helicase which initiates the ICL repair [8]. Finally, it has been described that particular orientation of the Ap-ICL site within the DNA fork is necessary for sufficient removal

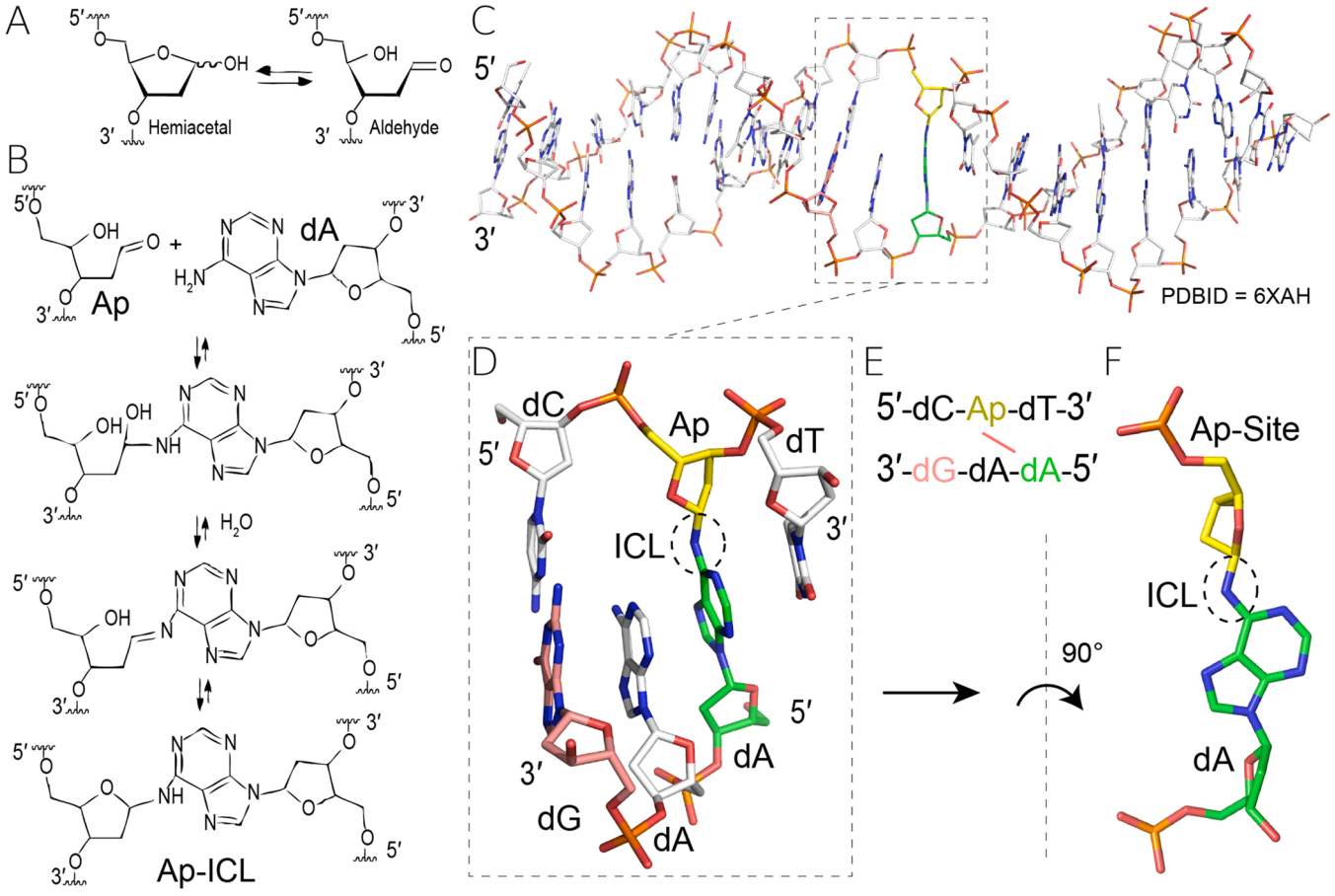

Fig. 1. Structure, sequence and formation of the Ap-ICL.A) The Ap site in an open and closed form, B) schematics of formation of Ap-ICL. C) The NMR model of the structure of Ap-ICL. D). An enlarged side view of the Ap-ICL within the duplex DNA with orphaned bases (Ap site in yellow, dG which is known to also form Ap-ICL in pink, and crosslinked adenine in green), E) the DNA sequence schematics in the vicinity of Ap-ICL in this NMR structure, and F) top view of the Ap-ICL crosslink (C-F) [45].(For interpretation of the references to colour in this figure, the reader is referred to the web version of this article.)

of the Ap-ICL [48]. The knowledge regarding the feasibility and prevalence of the Ap-ICL, however, remains elusive. Moreover, the circumstances such as the local sequence leading to formations and its kinetics are also only fragmental.

Here, we aim to reveal a sequence of contexts and conditions leading to the formation of the Ap-ICL *in vitro* and to predict the relevance, frequency and feasibility of Ap-ICL formation *in vivo*. With this goal in mind, we designed a panel of DNA oligonucleotides to study the rate of formation of Ap-ICL *in vitro* with regard to the sequence context. Our data reveal that individual changes in nucleobases surrounding Ap-ICLs influence the rate of formation of the Ap-site, but only to a certain extent. Significant changes in formation rates have been observed for Ap-ICLs generated within the duplex with AT-rich regions surrounding the crosslink lesion. We then followed the stability of the purified Ap-ICLs, and from our biochemical experiments regarding the formation of Ap-ICLs, we have estimated a theoretical number of Ap-ICLs formed in a living cell.

2. Materials and methods

2.1. Oligonucleotides for preparation of DNA containing native Ap site

All synthetic DNA oligonucleotides were acquired from (Sigma-Aldrich). Oligonucleotides for the preparation of native Ap sites were ordered with deoxy-uracil and were labelled with HEX (Table 1).

2.2. DNA crosslink formation

The reaction buffer for crosslinking reactions was optimized. The final reaction buffer was composed of 20 mM HEPES, pH = 6.5, 140 mM NaCl, 0.5 mM TCEP, and 5% glycerol. Comparative crosslinking experiments were carried out at Tris-HCl pH = 7.4, 140 mM NaCl and 5% glycerol to outline the similarity of results under physiological conditions (Supplementary Fig. S4). We mixed labelled DNA oligonucleotides with non-labelled complementary oligonucleotides 1:1 in an optimized buffer to the final DNA concentration of 2.5 μM. The DNA reaction mixture (50 μl) was annealed using Biometra Tprofessional Thermocycler by heating to 95 °C and then cooling to room temperature using the slowest ramp. For the Ap site creation, 0.5 U uracil-DNA glycosylase (UDG) (New England Biolabs) per one sequence reaction was added and kept 5 min at room temperature. Afterwards, UDG was inactivated with another round of an annealing cycle. The annealed DNA reaction mixture containing the Ap site was incubated for the duration of the experiment at 37 °C. At given time points, 1 ul of the crosslinking reaction was taken and mixed with 9 ul of formamide to stop the reaction. The stopped reaction was separated on a 20% denaturing polyacrylamide gel (1 x TBE, 7 M Urea 20% polyacrylamide: bisacrylamide 19:1) and visualized using a 532 nm laser and using a Cy3 570BP20 filter on an Amersham Typhoon Biomolecular Imager (GE Healthcare). The progress of the crosslinking reaction was quantified using a commercial ImageQuant TL. All bands in the individual lanes (substrate, product and intermediates) were densitometrically quantified to determine the percentage of the crosslink formed, the methodology was described previously in detail [49]. Control reaction with thymine in place of uracil to prevent Ap-ICL reaction was carried out with and without UDG, this control aimed to demonstrate the specificity of crosslinking at Ap site (Supplementary Fig. S2).

2.3. Isolation of crosslinked DNA from polyacrylamide gel for further reactions

Ap-ICL crosslink was purified from the PAGE gel using the modified band excision method from the gel [50]. The sample of crosslinked DNA was run on a 20% denaturing polyacrylamide gel. Bands were visualized using HeroLab UVT-20 S/M/L, and a band of crosslinked DNA was cut out, chopped and transferred to a tube with 200 μl of elution buffer (20 mM Tris, pH 7.4, 140 mM NaCl, 0.5 mM TCEP, 5% glycerol). The tube was left on a rotating wheel at 8 °C overnight. The sample was then centrifuged at 800 g for 1 min. The remaining buffer was recovered and purified using Cytiva MicroSpin™ G-25 Columns against the elution buffer to remove excess urea. The final sample of purified Ap-ICL DNA was run on 20% denaturing polyacrylamide gel to verify its purity.

2.4. Analysis of degradation of crosslinked DNA

The stability of crosslinked DNA was assessed at 37 °C in 20 mM Tris, pH 7.4, 140 mM NaCl, 0.5 mM TCEP, 5% glycerol. At given time points, typically 1 day, 2 μl of a solution of crosslinked DNA was taken, 8 μl of

Table 1
DNA oligonucleotide sequences. Sequences of dsDNA oligonucleotides, and their names used in this study. Ap site is generated from uracil (U) on the position 2 and Ap-ICL forms with adenine on the position 6, the reaction confirming the specificity of Ap-ICL crosslinking reaction is shown in Supplementary Fig. S3.

4G	5′[HEX]-GTCGATGAAC$_1$**U$_2$**T$_3$AGACAGCT 3′-CAGCTACTT**G$_4$**A$_5$**A$_6$**TCTGTCGA	4I	5′[HEX]-GTCGATGAAC$_1$**U$_2$**T$_3$AGACAGCT 3′-CAGCTACTT**I$_4$**A$_5$**A$_6$**TCTGTCGA
4C	5′[HEX]-GTCGATGAAC$_1$**U$_2$**T$_3$AGACAGCT 3′-CAGCTACTT**C$_4$**A$_5$**A$_6$**TCTGTCGA	6I	5′[HEX]-GTCGATGAAC$_1$**U$_2$**T$_3$AGACAGCT 3′-CAGCTACTTG$_4$A$_5$**I$_6$**TCTGTCGA
4T	5′[HEX]-GTCGATGAAC$_1$**U$_2$**T$_3$AGACAGCT 3′-CAGCTACTT**T$_4$**A$_5$**A$_6$**TCTGTCGA		
4(5)A	5′[HEX]-GTCGATGAAC$_1$**U$_2$**T$_3$AGACAGCT 3′-CAGCTACTT**A$_4$**A$_5$**A$_6$**TCTGTCGA	TT	5′[HEX]-GTCAGATC**AAA$_1$U$_2$**T$_3$**AA**ACCTG 3′-CAGTCTAG**TTT$_4$**G$_5$**A$_6$TT**TGGAC
5G	5′[HEX]-GTCGATGAAC$_1$**U$_2$**T$_3$AGACAGCT 3′-CAGCTACTTA$_4$**G$_5$A$_6$**TCTGTCGA	TC	5′[HEX]-GTCAGATC**AAG$_1$U$_2$**T$_3$**AA**ACCTG 3′-CAGTCTAG**TTC$_4$**G$_5$**A$_6$TT**TGGAC
5C	5′[HEX]-GTCGATGAAC$_1$**U$_2$**T$_3$AGACAGCT 3′-CAGCTACTTA$_4$**C$_5$A$_6$**TCTGTCGA	GT	5′[HEX]-GTCAGATC**CCA$_1$U$_2$**T$_3$**CC**ACCTG 3′-CAGTCTAG**GGT$_4$**G$_5$**A$_6$GG**TGGAC
5T	5′[HEX]-GTCGATGAAC$_1$**U$_2$**T$_3$AGACAGCT 3′-CAGCTACTTA$_4$**T$_5$A$_6$**TCTGTCGA	GC	5′[HEX]-GTCAGATC**CCG$_1$U$_2$**T$_3$**CC**ACCTG 3′-CAGTCTAG**GGC$_4$**G$_5$**A$_6$GG**TGGAC

formamide was added, and the sample was frozen at −80 °C to terminate the degradation. After that, all samples were resolved on 20% denaturing polyacrylamide gel to validate the progress of degradation. The gel was scanned using a laser at 532 nm and a Cy3 570BP20 filter on the Amersham Typhoon Biomolecular Imager (GE Healthcare). The image was analyzed using the commercial ImageQuant TL. Lines were selected manually, and the background subtraction was performed using the rolling ball method. Bands with constant dimensions encompassing crosslinked DNA and degradation products were selected manually. For every line, the percentage of degradation of crosslinked DNA was calculated based on the ratio of the remaining crosslinked DNA and the degradation product.

3. Results

3.1. Design of the DNA substrates

Uracil, and thus the Ap site, was situated in the middle of the oligonucleotide duplex. All residues in the vicinity were named accordingly (Fig. 2A), and the position of the Ap site was numbered 2. The base to which the majority of crosslinks is formed was fixed to be adenine at position 6 [36]. Therefore, in our experimental setup, positions 2 and 6 were constant as there were involved in the Ap-ICL formation with the exception of a control experiment validating the preferential formation of these sites. Only natural DNA nucleobases were altered in other positions to obtain all possible combinations in the vicinity of the Ap site. Position 5 is opposite to the Ap site lesion. Because positions 1 and 4 were intrinsically linked by complementarity, thereafter the experiments were focused on positions 4 and 5. Subsequently, a wider area of the Ap site was investigated with the specific goal of comparing the AT-rich and GC-rich regions (Fig. 3).

3.2. Generation of the Ap site and crosslink formation

Purchased synthetic DNA oligonucleotides contained deoxyuridine and were labelled with 5′ fluorescent dye (HEX, 6-hexachloro-fluorescein). Uracils were introduced to easily generate a native Ap site. First, the oligos were annealed with a complementary DNA strand and

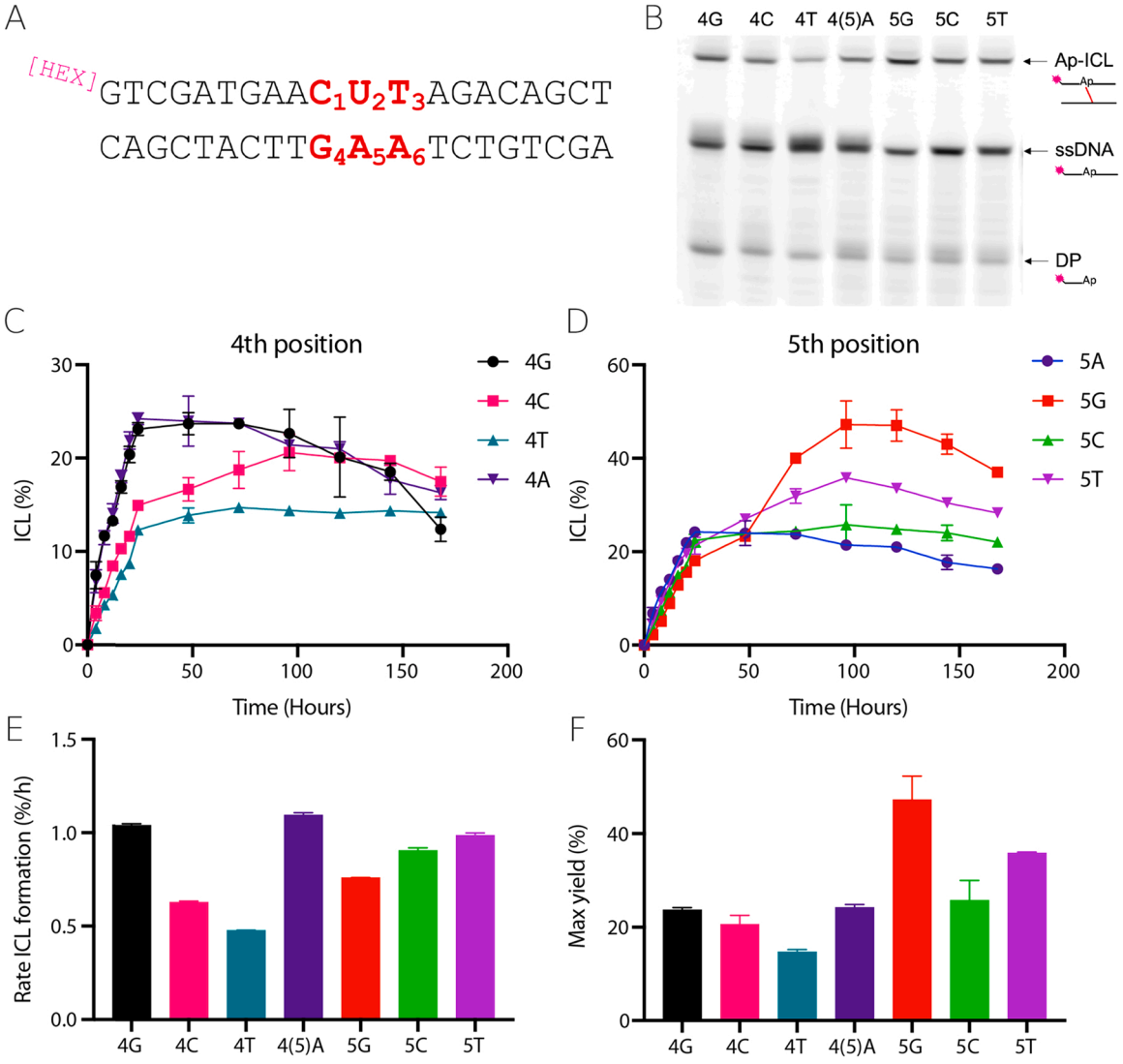

Fig. 2. Reaction kinetics of the Ap site DNA when varying bases at positions 4 and 5, respectively.*(A) Schematic design of the DNA duplex containing the Ap site and nomenclature of different positions. Position 2 is where the Ap site is formed by reaction with UDG, and ICL is formed between positions 2 and 6. Reactions were initiated by the formation of the Ap site by UDG and kept in dark at 37 °C (B) Reactions in each timepoint were stopped (here 24 h) and immediately resolved on 20% denaturing PAGE gel, ssDNA marks single-stranded DNA and DP donates degradation product. The gels were evaluated and the proportion of Ap-ICL formed from DNA oligos with different nucleobase in position 4(C) or position 5(D) were plotted in the graph. The initial rates of Ap-ICL formation (E) and the maximum yield (F) of Ap-ICL we plotted as bar charts. Error bars represent SEM from three independent repeats. Comparative gel at Tris-HCl pH = 7.4, 140 mM NaCl shown in the* Supplementary Fig. S4.

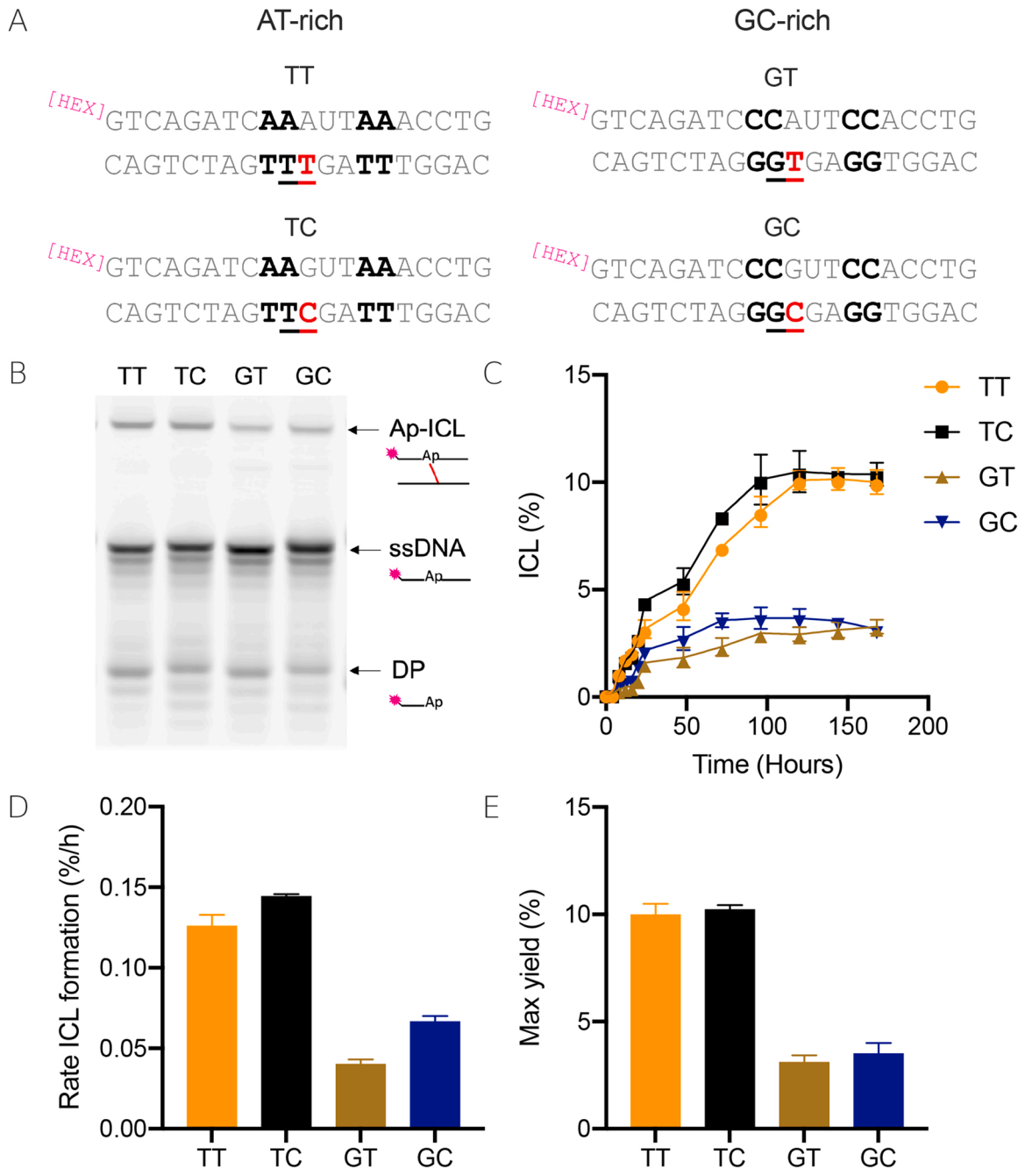

Fig. 3. Formation of Ap-ICL in DNA duplexes with AT-rich or GC-rich regions. *(A) Schematics of DNA duplexes containing i) AT-rich regions (left) or ii) GC-rich regions (right), in the vicinity of the Ap site. AT-rich sequences where thymine and cytosine are interchanged in the 4th position are named TT or TC; similarly, GC-rich sequences with bases in the 4th position are named GT or GC. (B) Reactions were resolved on 20% denaturing PAGE gel, ssDNA marks single-stranded DNA and DP donates degradation product. (C) Reaction kinetics of Ap-ICL formation from DNA oligos with AT-rich or GC-rich regions. The rate of ICL formation (D) and the maximum yield (E) were plotted for all four sequences. Error bars represent SEM from four independent repeats.*

incubated with an UDG [51,52]. The minimal amount of this enzyme was estimated by its titration into the reaction mixture. The presence of the generated Ap site was monitored on the PAGE gel after its sufficient hydrolysis by NaOH at an elevated temperature (Supplementary Fig. S1). Typically, a 5 min incubation with UDG was sufficient for a total conversion of the uracil to the Ap site.

The crosslinking reaction was allowed to proceed in a dark incubator at 37 °C. Aliquots were taken at different time points to monitor the time course. The fluorescently labelled samples were analyzed on denaturing PAGE gels, imaged, quantified and the percentage of generated crosslink was plotted in a graph. Initial rates were calculated as a linear fit to the data and maximum yields of Ap-ICL were determined as the maximum measured value.

3.3. The opposite nucleotide to the Ap site influences the rate of formation of Ap-ICL

The chemical nature of the DNA is as such that Ap sites can be generated spontaneously at any given DNA context [30]. In our first set of experiments, the single base opposing the Ap site was varied whilst the sequence of the entire remaining DNA duplexed was identical. In this setup, all four bases were tested on this position that we named the 5th

position (Fig. 2A), The rate of formation of Ap-ICLs were followed so as the maximum yields. The data were plotted in the graph and to bar charts. The observed rates were 1.1%/h for 5 A, 0.76%/h for 5 G, 0.91%/h for 5 C and 0.99%/h for 5 T (we took the liberty to express the rates in the percentage of original Ap sites converted in one hour to Ap-ICL). The maximum yield for all these oligos was 24.25% for 5 A, 47.2% for 5 G, 25.8% for 5 C and 35.9% for 5 T of the total DNA (For further rates please refer to Supplementary Tables ST1 – ST3). Later, with an increasing amount of degradation product, the amount of Ap-ICL started to decline. There were significant differences in the rate of formation as shown in the graph. Overall, these changes were relatively small and regardless of the nucleobase present opposite to the Ap site the Ap-ICL formed to a similar extent (Fig. 2).

3.4. Varying base-pair adjacent to Ap site on its 5′ end

Similar to the variation of the bases opposite to the AP site, the adjacent base-pair occupying positions 1 and 4 were varied. All four base pair combinations were tested for these positions and DNA oligonucleotides were named 4 G, 4 T, 4 C, and 4(5)A. Sequences 4 A and 5 A are identically co-named 4(5)A as 4 A was kept constant at 5th position and *vice-versa* with sequence 5 A. Yet again, significant differences in the formation of the Ap-site crosslink were observed. Surprisingly enough, the differences in rates of formation were not extraordinary, but the Ap-ICL was yet again formed in all possible base combinations. Overall, the rates vary approximately 2-fold (Supplementary Table ST1). The maximum yield varies slightly, and it was reached at different timepoints (Fig. 2 & ST1). The initial rate was the lowest for both pyrimidine bases. Both thymine and cytosine containing duplexes reached their maximum yield of crosslinks later but the percentages were not dissimilar with the remaining two bases at this position. Once again the amount of crosslinks starts to decline due to the irreversible decomposition to smaller degradation products (Fig. 2). To confirm published work and demonstrate the specificity of Ap-ICL forming from Ap with adenine residues, two control experiments were carried out. For sequence 4 G, hypoxanthine was placed at positions 4 and 6. No visible Ap-G crosslink was formed when adenine at position 6 was mutated to hypoxanthine. In contrast, when hypoxanthine was placed at position 4, however, Ap-A crosslink was formed as readily as when guanine was present (Fig. SI 3).

3.5. AT-rich regions facilitate Ap-ICL formation

Investigating the sequence surrounding the Ap site has revealed the differences in the rate of Ap-ICL formation, although a more complete picture requires investigation of further sequence variation that may influence the rigidity of the entire region encompassing the Ap site. We modified the sequence in the wider surrounding of the Ap site by a set of two AT or GC pairs from both sites (Fig. 3A). We set out to determine how AT-rich and GC-rich sequences influence the rate of formation of Ap-ICL. These sequences were tested in non-identical duplicates for which the base at 4th position contained either cytosine or thymine and the oligos were named accordingly (TT, TC, GT, GC), *e.g.* TC is an AT-rich oligonucleotide with C at 4th position (Fig. 3A). These bases were chosen to extend the AT-rich or GC-rich part around the Ap-site. The reaction set-up was identical as above, where reaction progress was monitored on a denaturing PAGE gel. The amount of formed Ap-ICL was apparent from the gel figures (Fig. 3B). Next, the gels were evaluated, and initial reaction rates were determined from the slopes of the data points.

When AT- and GC-rich regions were swapped, we observed significant differences in the rate of formation (Fig. 3C). The effect of the cytosine or thymine base at the 4th position on the rate of the reaction is rather small and the rates for oligos containing cytosine were faster than those with thymine. This was observed for both AT-rich and GC-rich DNA duplexes, and this trend was consistent in experiments shown in Fig. 2 and Fig. 3 confirming the robustness of our approach. Finally, the rate of formation for the AT-rich sequence with a cytosine at 4th position (TC) had a nearly 4 times higher rate of formation than the one with GC-rich sequence with thymine at 4th position (GT). This trend was observed for both pairs of sequences (TC > TT >>> GC > GT), and it was also reflected in a maximum yield reaching an approximate 2.5-fold difference (Fig. 3E).

3.6. Stability of Ap-ICL

Finally, the stability of Ap-ICL was tested to determine how persistent the crosslink could be at physiological conditions and without the intervention of other proteins and enzymes. The Ap-ICLs were purified by isolation from the gel. Large volumes of the crosslinking reactions stopped approximately at the timepoint for the maximum yield of the Ap-ICL. After their isolation, the pure Ap-ICLs were buffer-exchanged into a physiological buffer and subjected to their spontaneous decomposition. Our initial experiments as well as published literature have suggested that the decomposition of Ap-ICL is a lengthy process [53]. Therefore, the subsamples were taken in 24 h intervals, and after two weeks, all reaction time points were resolved on denaturing PAGE gels (Fig. 4 A). The proportions of degrading Ap-ICL were plotted as a function of time, the initial reaction rates of their decomposition were fitted with single exponential decay and plotted into a bar chart (Fig. 4B & 4 C). The ICL band disintegrated into a band the size of the original substrate. With a delay, more products appeared, with the nature of these substrates arising from the spontaneous hydrolysis of the Ap site. Sequences with AT- and GC-rich regions were used in this experiment, and all reactions had a similar rate of decomposition, except for an AT-rich sequence with a T at the 4th position (TT) that decomposed at a slightly slower rate. Less than 1/5 of the initial material was decomposed in the first 10 days (Fig. 4).

4. Discussion

The first studies of specific Ap-ICL outlined two possible ways by which the Ap-ICL can form [2,37]. They demonstrated that within a duplex within this exemplary sequence 5′-dC-Ap-dT, Ap-ICL can be formed by crosslinking Ap with guanine or adenine in the opposite DNA strand. The latter study showed that an Ap-G crosslink is not stable unless reduced with $NaBH_3CN$. This is presumably due to its sterically unfavourable arrangement, and the crosslink reverted back to the Ap site. Importantly, and perhaps coincidentally, the identical sequence motif was used to determine the NMR structure of Ap-ICL within the DNA duplex. In this study, only one type of crosslink was observed, making a 5′Ap-dT "hotspot" of Ap site crosslink formation *in vivo* (Fig. 1) [36]. Recently, another Ap-ICL where Ap site linking amino group of cytosine from opposite DNA strand (Ap-C) was observed. This Ap-ICL was preferentially formed within where C was mispaired with A. This crosslink was only formed at quite acidic conditions pH = 5 and was shown not to form under physiological conditions in nonmispaired oligonucleotide [54].

In this manuscript, we focused on Ap-ICL formed within this 5′-Ap-dT "hot-spot". We have a synthesized and annealed panel of DNA oligonucleotides with different DNA sequences surrounding the Ap site. The entire study used this non-enzymatic Ap-ICL formation, and by measuring its kinetics, we revealed sequence circumstances and influences leading to the formation of ICLs. To investigate the generation of the Ap-ICL, uracil was converted to the Ap site by an enzymatic reaction with UDG. We then set up the reactions to measure the rates of ICL formation for individual oligonucleotides with different sequences. Reactions were terminated at different time points, resolved on PAGE gels and the fractions of crosslinks formed were plotted against time. This allowed us to follow the kinetics of ICL formation. Our data has revealed that different nucleotides surrounding the Ap site affected the rate of the Ap-ICL formation. Although the rates differed to an extent,

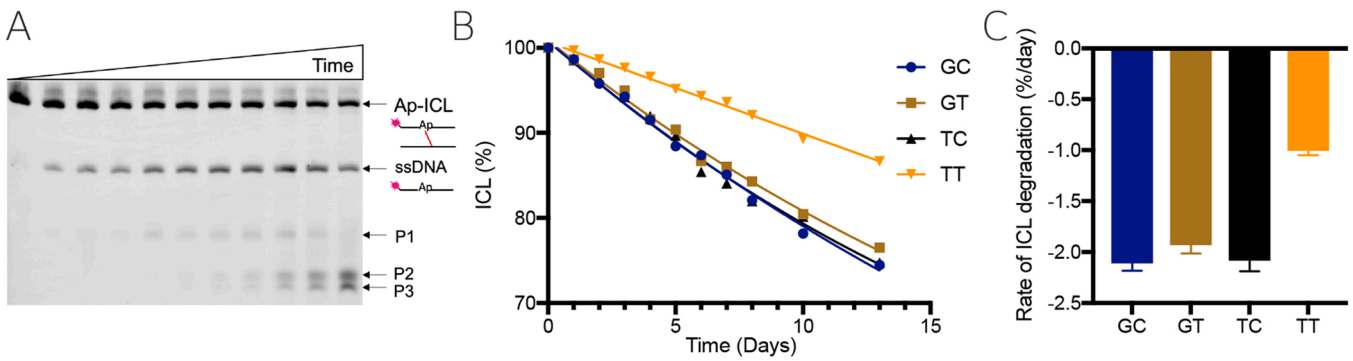

Fig. 4. Stability and degradation of Ap-ICL with AT-rich or GC-rich regions.*Gel purified Ap-ICLs from DNA oligos with AT-rich or GC-rich regions flanking the Ap site were subjected to spontaneous degradation at physiological conditions. (A) An illustrative 20% denaturing PAGE gel of Ap-ICL degradation in time is shown, where P1, P2 and P3 are products of degradation. HEX-labelled fluorescent imaging. (B) Degradation of Ap-ICL was plotted over time and fitted with exponential decay (C) The rate of Ap-ICL degradation was plotted and is represented as a bar chart. The half-lives for GC, GT, TC and TT were 28.8; 31.7; 29.3 and 60.6 days.*

what we found most striking was that the Ap-ICLs form consistently within all of these sequences and that the resulting crosslinks were very stable with a half-life longer than 30 days. This is in agreement with the literature where different Ap-ICL were already been reported to be relatively stable [47,53–55].

The data show that the rate of formation of the Ap-ICLs is only slightly affected by different single nucleotide or one base pair substitutions in the vicinity of the Ap site. The maximum yield of Ap-ICLs for all of these sequences was roughly 15%. Meaning that on average 15% of Ap sites are converted into Ap-ICLs. On the other hand, the formation of ICLs is significantly affected by the presence of AT-rich or GC-rich regions flanking the Ap site. In the case of AT-rich sequences, we observed significantly higher rates of formation. We speculate that this may be because AT-rich regions have a lower melting temperature and thus allow for "DNA breathing". We predict that weaker base-pairing, in turn, would allow for crosslinking reactions to proceed with less difficulty and faster. Although our study is focused purely on the *in vitro*, non-enzymatic formation of Ap-ICLs, the study aimed to broaden understanding of which circumstances and how often the crosslinks can form *in vivo*. Below, we attempt to make a rough estimate on the number of Ap-ICLs in one human cell, as our work shed light on a rough number of Ap-ICLs formed per 100 Ap sites.

Spontaneous deamination and depurination generate 10,000 Ap/sites/day in a cell [13,14]. In addition to this, the DNA damage and action Ap site generation by various DNA glycosylases further increase this number [30]. To accurately count this number can be challenging. Our rough estimate disregards that DNA repair enzymes are present, and they eliminate the majority of Ap sites. Then, observable Ap sites at any given moment may only represent 0.25–4% of the sites that would form the Ap-ICL during the day. We may predict that the majority of these Ap sites are repaired or protected by the formation of DNA protein crosslinks, and therefore only a small proportion of Ap sites are present [53,56–58]. In recent work, a relative number of Ap-sites were estimated and compared against the knockdown of human Ap endonuclease APEX1. It has been observed that an extra 77% more Ap sites were present in the knockdown, while 90% of the enzyme was removed [59]. It is difficult to estimate the original numbers of Ap sites from this relative comparison, but these numbers suggest that significant numbers still persist in the genome.

With DNA fibre analysis, it was predicted that the number of Ap sites to be more than 35,000 Ap sites in one human cell [56]. On the other hand, further methods for determining the presence of Ap sites have been developed. A mass spectroscopy method using a chemical O-(pyridine-3-yl-methyl) hydroxylamine (PMOA) is reportedly a very sensitive technique for the detection of Ap sites directly within the duplex [60]. This technique is quantitative and allows for the detection of up to 2 Ap sites in 10^8 nt. With such sensitivity, a rough number of the steady-state Ap sites detected by this method is 2 Ap sites per 10^7 nt [61]. Considering that the human genome has 3.2×10^9 nt and is diploid, then one human cell would have only 160 Ap sites. It is noteworthy, that experiments using aldehyde reactive probes might be biased as the probe may react with other aldehydes in the DNA. The Ap site undergoes a mutarotation as do other sugar moieties, and generally, only less than 1% of the sugars are in open aldehyde form [33,35]. Therefore, the rate of derivatization of the Ap site with an aldehyde reactive probe will be determined by the ring-opening reaction of the ribose into the aldehyde form. The rate of ring-opening can be noticed in mass spectroscopy studies where PMOA reagent was used. Here, almost the full conversion of small DNA oligonucleotide containing Ap site to a PMOA adduct was shown on HPLC chromatograms and confirmed by mass spectroscopy [62]. Additionally, a biochemical study with an aldehyde reactive probe conjugated with biotin showed that the majority of Ap sites were conjugated with the probe if sufficient time and reagents were in supply [63]. Both studies with PMOA, including one with mammalian samples, used excessive amounts of PMOA allowing first-order kinetics where ring-opening of Ap site is a rate-limiting reaction. Thereafter, we believe that HPLC-MS detection of conjugated Ap-sites is specific and validated by the MS method and might be the most accurate. This leads to a steady-state value of only about 100–200 Ap sites present in the genome. Moreover, product inhibited bifunctional glycosylases may bind and crosslink the Ap-sites [32,64,65]. Other DNA repair enzymes and DNA binding proteins interacting with Ap sites could impede the Ap-ICL formation thus protecting the genome integrity [57,66,67]. Additionally, it has been also shown that Ap-ICL crosslink can be reverted beside the repair by NEIL3 glycosylase [7,53]. On the other hand, human Ap endonuclease and exonuclease APEX1 was shown to cleave the Ap-ICL using its exonuclease activity on degraded Ap-G crosslink. These protective processes could explain the relatively low number of Ap sites detected using PMOA and mass spectroscopy. Based on the aforementioned predictions and our data, we estimate the amount of Ap-ICL crosslink to be 1–5 Ap-ICLs present or formed in any human cell.

Author contribution

BL and AH designed, optimized and carried out experiments, AH designed figures, EB and JS supervised the study and wrote the manuscript.

Acknowledgements

This work was supported by the Czech Science Foundation (17–21649Y), and we thank the Academy of Sciences Czech Republic for support in the form of a J.E. Purkyne Fellowship awarded to JS. The

project was also supported by the Academy of Sciences Czech Republic (RVO: 61388963). We cordially acknowledge Edward Curtis and Tamara Jenkins for the critical reading and proofreading of the manuscript.

Appendix A. Supporting information

Supplementary data associated with this article can be found in the online version at doi:10.1016/j.dnarep.2022.103300.

References

[1] J. Zhang, J.C. Walter, Mechanism and regulation of incisions during DNA interstrand cross-link repair, DNA Repair 19 (2014) 135–142, https://doi.org/10.1016/j.dnarep.2014.03.018 ((Amst)).

[2] F. Coste, J.-M. Malinge, L. Serre, W. Shepard, M. Roth, M. Leng, C. Zelwer, Crystal structure of a double-stranded DNA decamer containing a cisplatin interstrand cross-link adduct, Nucleic Acids Res. 27 (1999) 1837–1846.

[3] D.M. Noll, T. McGregor Mason, P.S. Miller, Formation and repair of interstrand cross-links in DNA, Chem. Rev. 106 (2006) 277–301, https://doi.org/10.1021/cr040478b.

[4] K.M. Johnson, N.E. Price, J. Wang, M.I. Fekry, S. Dutta, D.R. Seiner, Y. Wang, K. S. Gates, On the formation and properties of interstrand DNA-DNA cross-links forged by reaction of an abasic site with the opposing guanine residue of 5′-CAp sequences in duplex DNA, J. Am. Chem. Soc. 135 (2013) 1015–1025, https://doi.org/10.1021/ja308119q.

[5] J. Nakamura, M. Nakamura, DNA-protein crosslink formation by endogenous aldehydes and AP sites, DNA Repair 88 (2020), 102806, https://doi.org/10.1016/j.dnarep.2020.102806 ((Amst)).

[6] M. Räschle, P. Knipsheer, M. Enoiu, T. Angelov, J. Sun, J.D. Griffith, T. E. Ellenberger, O.D. Schärer, J.C. Walter, Mechanism of replication-coupled DNA interstrand crosslink repair, Cell 134 (2008) 969–980, https://doi.org/10.1016/j.cell.2008.08.030.

[7] D.R. Semlow, J. Zhang, M. Budzowska, A.C. Drohat, J.C. Walter, Replication-dependent unhooking of DNA interstrand cross-links by the NEIL3 Glycosylase, e14, Cell 167 (2016) 498–511, https://doi.org/10.1016/j.cell.2016.09.008.

[8] R.A. Wu, D.R. Semlow, A.N. Kamimae-Lanning, O.V. Kochenova, G. Chistol, M.R. G. Hodskinson, R. Amunugama, J.L. Sparks, M. Wang, L. Deng, C.A. Mimoso, E. Low, K.J. Patel, J.C. Walter, TRAIP is a master regulator of DNA interstrand crosslink repair, Nature 567 (2019) 267–272, https://doi.org/10.1038/s41586-019-1002-0.

[9] P.R. Martin, S. Couvé, C. Zutterling, M.S. Albelazi, R. Groisman, B.T. Matkarimov, J.L. Parsons, R.H. Elder, M.K. Saparbaev, The human DNA glycosylases NEIL1 and NEIL3 excise psoralen-induced DNA-DNA cross-links in a four-stranded DNA structure, Sci. Rep. 7 (2017) 1–13, https://doi.org/10.1038/s41598-017-17693-4.

[10] P. Knipscheer, M. Räschle, A. Smogorzewska, M. Enoiu, T.V. Ho, O.D. Schärer, S. J. Elledge, J.C. Walter, The fanconi anemia pathway promotes replication-dependent DNA interstrand cross-link repair, Science 326 (2009) 1698–1701, https://doi.org/10.1126/science.1182372.

[11] M.R.G. Hodskinson, J. Silhan, G.P. Crossan, J.I. Garaycoechea, S. Mukherjee, C. M. Johnson, O.D. Schärer, K.J. Patel, Mouse SLX4 is a tumor suppressor that stimulates the activity of the nuclease XPF-ERCC1 in DNA crosslink repair, Mol. Cell. 54 (2014) 472–484, https://doi.org/10.1016/j.molcel.2014.03.014.

[12] M.R.G. Hodskinson, A. Bolner, K. Sato, A.N. Kamimae-Lanning, K. Rooijers, M. Witte, M. Mahesh, J. Silhan, M. Petek, D.M. Williams, J. Kind, J.W. Chin, K. J. Patel, P. Knipscheer, Alcohol-derived DNA crosslinks are repaired by two distinct mechanisms, Nature 579 (2020) 603–608, https://doi.org/10.1038/s41586-020-2059-5.

[13] T. Lindahl, B. Nyberg, Rate of depurination of native deoxyribonucleic acid, Biochemistry. 11 (1972) 3610–3618. ⟨http://www.ncbi.nlm.nih.gov/pubmed/4626532⟩.

[14] T. Lindahl, a Andersson, Rate of chain breakage at apurinic sites in double-stranded deoxyribonucleic acid, Biochemistry. 11 (1972) 3618–3623. ⟨http://www.ncbi.nlm.nih.gov/pubmed/4559796⟩.

[15] D. Svilar, E.M. Goellner, K.H. Almeida, R.W. Sobol, Base excision repair and lesion-dependent subpathways, Antioxid. Redox Signal. 14 (2011) 2491–2507.

[16] C.D. Mol, A.S. Arvai, R.J. Sanderson, G. Slupphaug, B. Kavli, H.E. Krokan, D. W. Mosbaugh, J.A. Tainer, Crystal structure of human uracil-DNA glycosylase in complex with a protein inhibitor: Protein mimicry of DNA, Cell 82 (1995) 701–708, https://doi.org/10.1016/0092-8674(95)90467-0.

[17] A.L. Ross, J.E. Sale, The catalytic activity of REV1 is employed during immunoglobulin gene diversification in DT40, Mol. Immunol. 43 (2006) 1587–1594, https://doi.org/10.1016/j.molimm.2005.09.017.

[18] C. Rada, G.T. Williams, H. Nilsen, D.E. Barnes, T. Lindahl, M.S. Neuberger, Immunoglobulin isotype switching is inhibited and somatic hypermutation perturbed in UNG-deficient mice, Curr. Biol. 12 (2002) 1748–1755, https://doi.org/10.1016/S0960-9822(02)01215-0.

[19] E.J. Steele, Mechanism of somatic hypermutation: critical analysis of strand biased mutation signatures at A:T and G:C base pairs, Mol. Immunol. 46 (2009) 305–320, https://doi.org/10.1016/j.molimm.2008.10.021.

[20] B. Demple, T. Herman, D.S. Chen, Cloning and expression of APE, the cDNA encoding the major human apurinic endonuclease: definition of a family of DNA repair enzymes, Proc. Natl. Acad. Sci. USA 88 (1991) 11450–11454, https://doi.org/10.1073/pnas.88.24.11450.

[21] D. Lu, J. Silhan, J.T. MacDonald, E.P. Carpenter, K. Jensen, C.M. Tang, G. S. Baldwin, P.S. Freemont, Structural basis for the recognition and cleavage of abasic DNA in Neisseria meningitidis, Proc. Natl. Acad. Sci. 109 (2012) 16852–16857, https://doi.org/10.1073/pnas.1206563109.

[22] M. Bhagwat, J. a Gerlt, 3'- and 5'-Strand cleavage reactions catalyzed by the Fpg protein from Escherichia coli occur via successive beta- and delta-elimination mechanisms, respectively, Biochemistry 35 (1996) 659–665, https://doi.org/10.1021/bi9522662.

[23] H.M. Nash, S.D. Bruner, O.D. Schärer, T. Kawate, T. a Addona, E. Spooner, W. S. Lane, G.L. Verdine, Cloning of a yeast 8-oxoguanine DNA glycosylase reveals the existence of a base-excision DNA-repair protein superfamily, Curr. Biol. 6 (1996) 968–980. ⟨http://www.ncbi.nlm.nih.gov/pubmed/8805338⟩.

[24] B. Demple, L. Harrison, Repair of oxidative damage to DNA: enzymology and biology, Annu. Rev. Biochem. 63 (1994) 915–948, https://doi.org/10.1146/annurev.bi.63.070194.004411.

[25] V. Bailly, W.G. Verly, AP endonucleases and AP lyases, Nucleic Acids Res. 17 (1989) 3617–3618. ⟨http://www.ncbi.nlm.nih.gov/pmc/articles/PMC317828/⟩.

[26] C.C. RICHARDSON, I.R. LEHMAN, A. KORNBERG, A deoxyribonucleic acid phosphatase-exonuclease from Escherichia coli, J. Biol. Chem. 239 (1964) 251–258.

[27] D.S. Chen, T. Herman, B. Demple, Two distinct human DNA diesterases that hydrolyze 3′-blocking deoxyribose fragments from oxidized DNA, Nucleic Acids Res. 19 (1991) 5907–5914, https://doi.org/10.1093/nar/19.21.5907.

[28] L. Wiederhold, J.B. Leppard, P. Kedar, F. Karimi-Busheri, A. Rasouli-Nia, M. Weinfeld, A.E. Tomkinson, T. Izumi, R. Prasad, S.H. Wilson, S. Mitra, T. K. Hazra, AP endonuclease-independent DNA base excision repair in human cells, Mol. Cell. 15 (2004) 209–220, https://doi.org/10.1016/j.molcel.2004.06.003.

[29] J. Silhan, Q. Zhao, E. Boura, H. Thomson, A. Förster, C.M. Tang, P.S. Freemont, G. S. Baldwin, Structural basis for recognition and repair of the 3′-phosphate by NExo, a base excision DNA repair nuclease from Neisseria meningitidis, Nucleic Acids Res. 46 (2018) 11980–11989, https://doi.org/10.1093/nar/gky934.

[30] D.E. Barnes, T. Lindahl, Repair and genetic consequences of endogenous DNA base damage in mammalian cells, Annu. Rev. Genet. 38 (2004) 445–476, https://doi.org/10.1146/annurev.genet.38.072902.092448.

[31] A. Álvarez-Quilón, J.L. Wojtaszek, M. Mathieu, T. Patel, C.D. Appel, N. Hustedt, S. E. Rossi, B.D. Wallace, D. Setiaputra, S. Adam, Y. Ohashi, H. Melo, T. Cho, C. Gervais, I.M. Muñoz, E. Grazzini, J.T.F. Young, J. Rouse, M. Zinda, R. S. Williams, D. Durocher, Endogenous DNA 3′ blocks are vulnerabilities for BRCA1 and BRCA2 deficiency and are reversed by the APE2 nuclease, Mol. Cell. (2020) 1–14, https://doi.org/10.1016/j.molcel.2020.05.021.

[32] R. Gilboa, D.O. Zharkov, G. Golan, A.S. Fernandes, S.E. Gerchman, E. Matz, J. H. Kycia, A.P. Grollman, G. Shoham, Structure of formamidopyrimidine-DNA glycosylase covalently complexed to DNA, J. Biol. Chem. 277 (2002) 19811–19816, https://doi.org/10.1074/jbc.M202058200.

[33] K.-S. Ryu, C. Kim, I. Kim, S. Yoo, B.-S. Choi, C. Park, NMR application probes a novel and ubiquitous family of enzymes that alter monosaccharide configuration, J. Biol. Chem. 279 (2004) 25544–25548, https://doi.org/10.1074/jbc.M402016200.

[34] C. De Los Santos, M. El-khateeb, P. Rege, K. Tian, F. Johnson, Impact of the C1′ configuration of abasic sites on DNA duplex structure, Biochemistry 43 (2004) 15349–15357, https://doi.org/10.1021/bi048400c.

[35] J.A. Wilde, P.H. Bolton, A. Mazumder, M. Manoharan, J.A. Gerlt, Characterization of the equilibrating forms of the aldehydic abasic site in duplex DNA by 17O NMR, J. Am. Chem. Soc. 111 (1989) 1894–1896, https://doi.org/10.1021/ja00187a062.

[36] S. Dimitrov, Y. Koleva, T.W. Schultz, J.D. Walker, O. Mekenyan, Interspecies quantitative structure-activity relationship model for aldehydes: aquatic toxicity, Environ. Toxicol. Chem. 23 (2004) 463–470, https://doi.org/10.1897/02-579.

[37] I.G. Minko, I.D. Kozekov, T.M. Harris, C.J. Rizzo, R.S. Lloyd, M.P. Stone, Chemistry and biology of DNA containing 1,N2-deoxyguanosine adducts of the α,β-unsaturated aldehydes acrolein, crotonaldehyde, and 4-hydroxynonenal, Chem. Res. Toxicol. 22 (2009) 759–778, https://doi.org/10.1021/tx9000489.

[38] H.-S. Yu, T. Oyama, T. Isse, K. Kitagawa, T.-T.-P. Pham, M. Tanaka, T. Kawamoto, Formation of acetaldehyde-derived DNA adducts due to alcohol exposure, Chem. Biol. Interact. 188 (2010) 367–375, https://doi.org/10.1016/j.cbi.2010.08.005.

[39] E. Freese, M. Cashel, Crosslinking of deoxyribonucleic acid by exposure to low pH, BBA Spec. Sect. Nucleic Acids Relat. Subj. 91 (1964) 67–77, https://doi.org/10.1016/0926-6550(64)90171-9.

[40] J. Burnotte, W.G. Verly, Crosslinking of methylated DNA by moderate heating at neutral pH, Biochim. Biophys. Acta Nucleic Acids Protein Synth. 262 (1972) 449–452, https://doi.org/10.1016/0005-2787(72)90488-1.

[41] C. Goffin, W.G. Verly, Interstrand DNA crosslinks due to AP (apurinic/apyrimidinic) sites, FEBS Lett. 161 (1983) 140–144, https://doi.org/10.1016/0014-5793(83)80747-9.

[42] C. Goffin, S. Bricteux-Grégoire, W.G. Verly, Some properties of the interstrand crosslinks in depurinated DNA, Biochim. Biophys. Acta Gene Struct. Expr. 783 (1984) 1–5, https://doi.org/10.1016/0167-4781(84)90071-X.

[43] A.S. Prakash, N.W. Gibson, Sequence-selective depurination, DNA interstrand cross-linking and DNA strand break formation associated with alkylated DNA, Carcinogenesis 13 (1992) 425–431, https://doi.org/10.1093/carcin/13.3.425.

[44] S. Dutta, G. Chowdhury, K.S. Gates, Interstrand cross-links generated by abasic sites in duplex DNA, J. Am. Chem. Soc. 129 (2007) 1852–1853, https://doi.org/10.1021/ja067294u.

[45] A.H. Kellum, D.Y. Qiu, M.W. Voehler, W. Martin, K.S. Gates, M.P. Stone, Structure of a stable interstrand DNA cross-link involving a β- N-Glycosyl Linkage between an N6-dA amino group and an abasic site, Biochemistry 60 (2021) 41–52, https://doi.org/10.1021/acs.biochem.0c00596.

[46] N.E. Price, K.M. Johnson, J. Wang, M.I. Fekry, Y. Wang, K.S. Gates, Interstrand DNA-DNA cross-link formation between adenine residues and abasic sites in duplex dna, J. Am. Chem. Soc. 136 (2014) 3483–3490, https://doi.org/10.1021/ja410969x.
[47] N.E. Price, M.J. Catalano, S. Liu, Y. Wang, K.S. Gates, Chemical and structural characterization of interstrand cross-links formed between abasic sites and adenine residues in duplex DNA, Nucleic Acids Res. 43 (2015) 3434–3441, https://doi.org/10.1093/nar/gkv174.
[48] M. Imani Nejad, K. Housh, A.A. Rodriguez, T. Haldar, S. Kathe, S.S. Wallace, B. F. Eichman, K.S. Gates, Unhooking of an interstrand cross-link at DNA fork structures by the DNA glycosylase NEIL3, DNA Repair 86 (2020), 102752, https://doi.org/10.1016/j.dnarep.2019.102752 ((Amst)).
[49] B. Cihlova, A. Huskova, J. Böserle, R. Nencka, E. Boura, J. Silhan, High-throughput fluorescent assay for inhibitor screening of proteases from rna viruses, Molecules 26 (2021), https://doi.org/10.3390/molecules26133792.
[50] A.M. Maxam, W. Gilbert, A new method for sequencing DNA, Proc. Natl. Acad. Sci. 74 (1977) 560–564, https://doi.org/10.1073/pnas.74.2.560.
[51] T. Lindahl, An N-Glycosidase from Escherichia coli That Releases Free Uracil from DNA Containing Deaminated Cytosine Residues, Proc. Natl. Acad. Sci. 71 (1974) 3649–3653, https://doi.org/10.1073/pnas.71.9.3649.
[52] S.R.W. Bellamy, G.S. Baldwin, A kinetic analysis of substrate recognition by uracil-DNA glycosylase from herpes simplex virus type 1, Nucleic Acids Res. 29 (2001) 3857–3863.
[53] S.J. Admiraal, P.J. O'Brien, Base excision repair enzymes protect abasic sites in duplex DNA from interstrand cross-links, Biochemistry 54 (2015) 1849–1857, https://doi.org/10.1021/bi501491z.
[54] M.J. Catalano, S. Liu, N. Andersen, Z. Yang, K.M. Johnson, N.E. Price, Y. Wang, K. S. Gates, Chemical structure and properties of interstrand cross-links formed by reaction of guanine residues with abasic sites in duplex DNA, J. Am. Chem. Soc. 137 (2015) 3933–3945, https://doi.org/10.1021/jacs.5b00669.
[55] J.G. Varela, L.E. Pierce, X. Guo, N.E. Price, K.M. Johnson, Z. Yang, Y. Wang, K. S. Gates, Interstrand cross-link formation involving reaction of a mispaired cytosine residue with an abasic site in duplex DNA, Chem. Res. Toxicol. 34 (2021) 1124–1132, https://doi.org/10.1021/acs.chemrestox.1c00004.
[56] P.D. Chastain, J. Nakamura, S. Rao, H. Chu, J.G. Ibrahim, J.A. Swenberg, D. G. Kaufman, Abasic sites preferentially form at regions undergoing DNA replication, FASEB J 24 (2010) 3674–3680, https://doi.org/10.1096/fj.09-145276.
[57] K.N. Mohni, S.R. Wessel, R. Zhao, A.C. Wojciechowski, J.W. Luzwick, H. Layden, B. F. Eichman, P.S. Thompson, K.P.M. Mehta, D. Cortez, HMCES maintains genome integrity by shielding abasic sites in single-strand DNA, Cell 176 (2019) 144–153, https://doi.org/10.1016/j.cell.2018.10.055, e13.
[58] S. Boiteux, F. Coste, B. Castaing, Repair of 8-oxo-7,8-dihydroguanine in prokaryotic and eukaryotic cells: properties and biological roles of the Fpg and OGG1 DNA N-glycosylases, Free Radic. Biol. Med. 107 (2017) 179–201, https://doi.org/10.1016/j.freeradbiomed.2016.11.042.
[59] N. Wang, H. Bao, L. Chen, Y. Liu, Y. Li, B. Wu, H. Huang, Molecular basis of abasic site sensing in single-stranded DNA by the SRAP domain of E. coli yedK, Nucleic Acids Res. 47 (2019) 10388–10399, https://doi.org/10.1093/nar/gkz744.
[60] K.P. Roberts, J.A. Sobrino, J. Payton, L.B. Mason, R.J. Turesky, Determination of Apurinic/Apyrimidinic Lesions in DNA with High-Performance Liquid Chromatography and Tandem Mass Spectrometry, Chem. Res. Toxicol. 19 (2006) 300–309, https://doi.org/10.1021/tx0502589.
[61] J. Guo, H. Chen, P. Upadhyaya, Y. Zhao, R.J. Turesky, S.S. Hecht, Mass SPectrometric Quantitation of Apurinic/Apyrimidinic Sites in Tissue DNA of Rats Exposed to Tobacco-Specific Nitrosamines and in Lung and Leukocyte DNA of Cigarette Smokers and Nonsmokers, Chem. Res. Toxicol. 33 (2020) 2475–2486, https://doi.org/10.1021/acs.chemrestox.0c00265.
[62] H. Chen, L. Yao, C. Brown, C.J. Rizzo, R.J. Turesky, Quantitation of apurinic/apyrimidinic sites in isolated DNA and in Mammalian tissue with a reduced level of artifacts, Anal. Chem. 91 (2019) 7403–7410, https://doi.org/10.1021/acs.analchem.9b01351.
[63] S. Bennett, J. Kitner, Characterization of the aldehyde reactive probe reaction with AP-sites in DNA: Influence of AP-lyase on adduct stability, Nucleosides Nucleotides Nucleic Acids 25 (2006) 823–842, https://doi.org/10.1080/15257770600726133.
[64] K. Nagorska, J. Silhan, Y. Li, V. Pelicic, P.S. Freemont, G.S. Baldwin, C.M. Tang, A network of enzymes involved in repair of oxidative DNA damage in Neisseria meningitidis, Mol. Microbiol. 83 (2012) 1064–1079, https://doi.org/10.1111/j.1365-2958.2012.07989.x.
[65] B. Landova, J. Silhan, Conformational changes of DNA repair glycosylase MutM triggered by DNA binding, FEBS Lett. 594 (2020) 3032–3044, https://doi.org/10.1002/1873-3468.13876.
[66] L.T. Da, J. Yu, Base-flipping dynamics from an intrahelical to an extrahelical state exerted by thymine DNA glycosylase during DNA repair process, Nucleic Acids Res. 46 (2018) 5410–5425, https://doi.org/10.1093/nar/gky386.
[67] P.S. Thompson, K.M. Amidon, K.N. Mohni, D. Cortez, B.F. Eichman, Protection of abasic sites during DNA replication by a stable thiazolidine protein-DNA cross-link, Nat. Struct. Mol. Biol. 26 (2019) 613–618, https://doi.org/10.1038/s41594-019-0255-5.